Separation Science and Technology
Publication details, including instructions for authors and subscription information:
http://www.informaworld.com/smpp/title~content=t713708471

Fluid Dynamics of Radial-Flow Ion Exchange in Partially Filled Columns

STUART H. MUNSON-McGEE[a]
[a] DEPARTMENT OF CHEMICAL ENGINEERING, NEW MEXICO STATE UNIVERSITY, LAS CRUCES, NEW MEXICO, USA

Online publication date: 27 November 2000

SEPARATION SCIENCE AND TECHNOLOGY, **35**(15), pp. 2415–2429, 2000

Fluid Dynamics of Radial-Flow Ion Exchange in Partially Filled Columns

STUART H. MUNSON-McGEE
DEPARTMENT OF CHEMICAL ENGINEERING
NEW MEXICO STATE UNIVERSITY
LAS CRUCES, NEW MEXICO 88003, USA

ABSTRACT

An experimental and numerical study demonstrated that completely filling the resin bed is essential if a radial-flow ion-exchange column is to work properly. The first phase of the study developed and verified a finite-element model of both an infinitely long column and finite-height column that was completely filled with resin. The porosity and tortuosity of the support columns of the ion-exchange column were calculated using a least-squares analysis of experimental pressure drop versus flow rate data in an empty column in conjunction with a theoretical analysis based on a layered-cylinder model. Numerical analysis of a partially filled column (i.e., one in which the top 2% of the resin bed was empty headspace) demonstrated that approximately 9% of the fluid would flow through the headspace. This fluid would never come in contact with the ion-exchange resin and would thus leave the column untreated. Modifying the column so that the top 10% of the support membranes was impermeable changed the flow lines such that the headspace was filled with a stagnant fluid and that, after this space was filled, all subsequent fluid entering the column flowed through the ion-exchange bed. This provides a method in which one could ensure that all the fluid would flow through the ion-exchange resin and be treated even if the column could not be or was not completely filled.

INTRODUCTION

A common method for removing trace contaminants from liquid streams is ion exchange. In the traditional ion-exchange process, the contaminated liquid is distributed over the top of a column of ion-exchange resin. The liquid passes down through the resin, typically coated polymeric beads, and the contaminant ion displaces a less harmful ion on the resin. This less-harmful ion be-

comes part of the liquid solution, thereby maintaining electrical neutrality in both the solution and the resin.

The contaminated liquid is allowed to flow through the resin bed until the resin is saturated with the contaminant ion. Then the flow of the contaminated liquid is halted and the resin washed with another liquid to remove the contaminant, replacing it with the original ion and restoring the resin to its original composition. The entire process can be repeated with additional contaminated liquid.

As described above, the principle flow of the contaminated liquid is vertically downward, giving rise to the descriptive name axial-flow ion exchange. Several difficulties can be encountered with this flow arrangement, including problems with scale-up from bench-scale studies to full-scale operation, excessive pressure drop across the resin bed, and channeling of the contaminated liquid along the walls of the column.

One proposed method for overcoming these problems is radial-flow ion exchange. In this process, the contaminated liquid is forced to flow radially through the ion-exchange resin. The resin is contained between two concentric annular porous tubes. The fluid is forced through the outer tube, through the ion-exchange resin, and then through the inner support tube into the inner annular region from which it is collected. This results in a shorter flow path through the ion-exchange resin and hence a lower pressure drop across the resin bed for a given flow rate. Scale-up from bench-scale to full-scale operation may also be easier since increasing the flow rate only requires a taller column but does not alter the fluid dynamics or the residence time for the contaminated resin in the ion-exchange resin bed itself, thus having no impact on the time the column can be used before the resin must be washed.

Several authors have studied the radial flow process. In early work, Lapidus and Amundson (1, 2) developed a mathematical model to describe mass-transport phenomena in a radial-flow bed of infinite thickness. They obtained reasonable agreement with experimental data from a wide range of conditions when diffusion in the liquid phase was assumed to be the rate-limiting step. Tsaur and Shallcross (3, 4) focused on the problems of mass transfer and radial dispersion and found reasonable agreement between their model and experimental data using a wedge-shaped column with the fluid flowing from the inside arc to the outside arc. Tharakan and Belizaire (5) compared the dispersion in axial- and radial-flow columns and determined that the radial-flow columns exhibited a larger dispersion than did the axial-flow columns with the fluid flowing from the outside to the inside.

The objective in studying this process was to evaluate its suitability for use in removing radioactive contaminants from aqueous solutions. In addition to characterizing the fluid dynamics and mass-transfer characteristics of a radial-flow column, there was interest in the potential for premature breakthrough and

ease of operation. Breakthrough occurs when the ion-exchange resin becomes saturated and the level of contamination in the discharged liquid exceeds the permissible level. If the fluid dynamics and mass-transfer characteristics are known sufficiently well, breakthrough can be estimated from theoretical analysis. Premature breakthrough occurs when contamination remains in the discharge liquid before the resin becomes saturated. This often happens due to maldistribution of the ion-exchange resin when the liquid channels down the side (in axial flow) or across the top (in radial flow) of the-ion exchange bed.

The principle components of this study are an experimental study to assess the ease of operation and characterize the porous tubes with respect to their permeability and tortuosity, and a theoretical and numerical study of the fluid dynamics for a layered porous structure in which the properties of the layers (i.e., the support tubes and the ion-exchange resin) could be varied along with the degree to which the intertube region was filled with ion-exchange resin. A follow-up study on the mass-transfer performance and estimating breakthrough curves for different operating conditions will be considered.

ANALYTICAL MODEL

A radial-flow ion-exchange column (Fig. 1) is characterized by an outer annulus through which the contaminated liquid is introduced into the column and an inner annulus from which the decontaminated liquid was collected. The inner support tube and outer support tube have interior and exterior radii of R_1, R_2, R_3, and R_4, respectively. The support tubes are assumed to have the same permeability and porosity. The ion-exchange resin, located between the two support tubes, is assumed to have its own porosity and permeability. To examine the effects of only partially filling the column with ion-exchange resin, the resin bed extends for $0 \leq z \leq h$ and an empty space is located above the resin bed, i.e., for $h \leq z \leq H$.

Fluid flow through each component of this composite, porous-material structure is described by the steady-state version of the conservation of mass

$$\nabla \cdot \mathbf{v} = 0 \tag{1}$$

and conservation of momentum (6)

$$\nabla \cdot \left(\frac{\rho \mathbf{v}\mathbf{v}}{\varepsilon} \right) + \nabla \mathbf{P} - \mu \nabla^2 \mathbf{v} + \mu F \mathbf{v} = 0 \tag{2}$$

where $\mathbf{v}$ is the velocity vector, $\mathbf{P}$ the hydraulic pressure, μ the viscosity, ρ the density, ε the porosity, and F the shear factor arising from flow through the porous media. In creeping flow the shear factor is given by (6)

$$F = 1/k \tag{3}$$

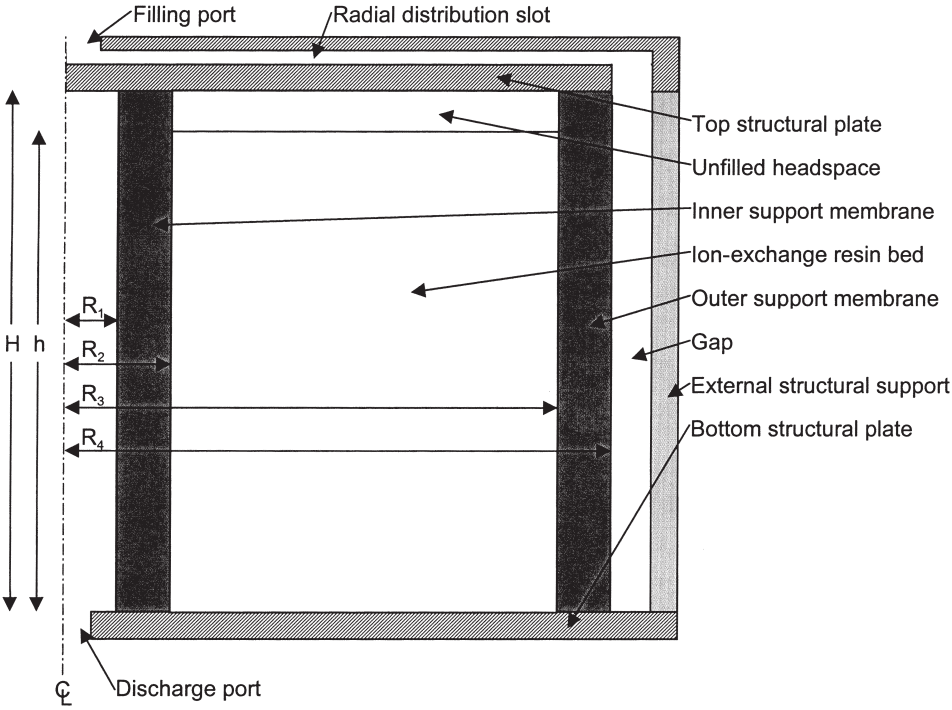

FIG. 1 Schematic diagram of the radial-flow ion-exchange column.

while for other cases it is given by

$$F = \frac{1}{k} + \frac{0.0081}{k} \frac{Re_k^2}{16^2 + Re_k^2} Re_k \tag{4}$$

where k is the material permeability and Re_k is the local modified Reynolds number given by

$$Re_k = 9.23 \frac{1 + (1 - \sqrt{\varepsilon})^{1/2}}{\varepsilon^2} \frac{\sqrt{k}\,\rho\,|\,\mathbf{v}\,|}{\mu} \tag{5}$$

In cylindrical coordinates, the mass conservation equation (assuming no variation with respect to angular position and a zero angular velocity) becomes

$$\frac{1}{r}\frac{\partial}{\partial r}(\rho r v_r) + \frac{\partial}{\partial z}(\rho v_z) = 0 \tag{6}$$

The radial and axial components of the momentum equation become

$$\frac{\rho}{\varepsilon}\left[v_r\frac{\partial v_r}{\partial r}+v_z\frac{\partial v_r}{\partial z}\right]+\frac{\partial P}{\partial r}-\mu\left[\frac{\partial}{\partial r}\left(\frac{1}{r}\frac{\partial}{\partial r}(rv_r)\right)+\frac{\partial^2}{\partial z^2}(v_r)\right]+\mu F v_r=0 \quad (7)$$

and

$$\frac{\rho}{\varepsilon}\left[v_r\frac{\partial v_z}{\partial r}+v_z\frac{\partial v_z}{\partial z}\right]+\frac{\partial P}{\partial z}-\mu\left[\frac{1}{r}\frac{\partial}{\partial r}r\left(\frac{\partial v_z}{\partial r}\right)+\frac{\partial^2 v_z}{\partial z^2}\right]+\mu F v_z=0 \quad (8)$$

For the special case of an infinitely long column, i.e., when H = ∞ and $v_z = 0$, the procedures of Bird et al. (7) can be followed to derive an expression for the velocity profile as a function of the difference between the pressure on the outside of the outer tube (P_4) and the pressure on the inside of the inside support tube (P_1) in terms of the geometry of the column, the properties of the supports and the ion-exchange resin, and the properties of the fluid. For this case, only the radial component of the continuity equation remains and is given by

$$\frac{\rho}{r}\frac{d}{dr}(rv_r)=0 \quad (9)$$

or

$$rv_r=\kappa \quad (10)$$

where κ is a constant. The radial component of the momentum equation becomes

$$\frac{\rho}{\varepsilon}\left[v_r\frac{dv_r}{dr}\right]+\frac{dP}{dr}+\mu F v_r=0 \quad (11)$$

Substituting (10) into (11) and evaluating the derivatives gives

$$-\frac{\rho\kappa^2}{\varepsilon r^2}+r\frac{dP}{dr}+\mu F\kappa=0 \quad (12)$$

For the case of creeping flow, i.e., when F is a constant, Eq. (12) can be rearranged and integrated to give

$$P_B-P_A=\left[-\frac{\rho\kappa^2}{2\varepsilon}\left(\frac{1}{R_B^2}-\frac{1}{R_A^2}\right)-\mu F\kappa\ln\left(\frac{R_B}{R_A}\right)\right] \quad (13)$$

where the subscripts A and B indicate two radial positions. For the three-layer ion-exchange column shown in Fig. 1, Eq. (13) can be used to determine the desired pressure-drop–velocity profile by applying it to each section individ-

ually and then eliminating the unknown pressures at the two interfaces, i.e., P_2 and P_3. The desired expressions are

$$P_4 - P_3 = \left[- \frac{\rho\kappa^2}{2\varepsilon_s} \left(\frac{1}{R_4^2} - \frac{1}{R_3^2} \right) - \mu F_s \kappa \ln\left(\frac{R_4}{R_3} \right) \right] \tag{14}$$

$$P_3 - P_2 = \left[- \frac{\rho\kappa^2}{2\varepsilon_{ix}} \left(\frac{1}{R_3^2} - \frac{1}{R_2^2} \right) - \mu F_{ix} \kappa \ln\left(\frac{R_3}{R_4} \right) \right] \tag{15}$$

$$P_2 - P_1 = \left[- \frac{\rho\kappa^2}{2\varepsilon_s} \left(\frac{1}{R_4^2} - \frac{1}{R_3^2} \right) - \mu F_s \kappa \ln\left(\frac{R_4}{R_3} \right) \right] \tag{16}$$

where the subscripts *s* and *ix* indicate the support tubes and the ion-exchange resin, respectively. Summing Eqs. (14)–(16) gives

$$\begin{aligned} P_4 - P_1 = & \left[- \frac{\rho\kappa^2}{2\varepsilon_s} \left(\frac{1}{R_4^2} - \frac{1}{R_3^2} + \frac{1}{R_2^2} - \frac{1}{R_1^2} \right) - \mu F_s \kappa \ln\left(\frac{R_4 R_2}{R_3 R_1} \right) \right] \\ & + \left[- \frac{\rho\kappa^2}{2\varepsilon_{ix}} \left(\frac{1}{R_3^2} - \frac{1}{R_2^2} \right) - \mu F_{ix} \kappa \ln\left(\frac{R_3}{R_2} \right) \right] \end{aligned} \tag{17}$$

which can be rearranged into a quadratic expression for κ

$$A\kappa^2 + B\kappa + C = 0 \tag{18}$$

with

$$A = \frac{\rho}{2\varepsilon_s} \left(\frac{1}{R_4^2} - \frac{1}{R_3^2} + \frac{1}{R_2^2} - \frac{1}{R_1^2} \right) + \frac{\rho}{2\varepsilon_{ix}} \left(\frac{1}{R_3^2} - \frac{1}{R_2^2} \right) \tag{19}$$

$$B = \mu F_s \left[\ln\left(\frac{R_4 R_2}{R_3 R_1} \right) \right] + \mu F_{ix} \ln\left(\frac{R_3}{R_2} \right) \tag{20}$$

$$C = P_4 - P_1 \tag{21}$$

FINITE ELEMENT ANALYSIS

A commercial finite-element analysis (FEA) program (8) was used to solve Eqs. (6)–(8). However, to decrease the number of elements and nodes generated by the program's self-meshing algorithm, the equations were first nondimensionalized with respect to R_4 in the radial direction and with respect to H in the axial direction. The resulting expressions were

$$H \frac{\partial}{\partial \hat{r}} (\rho \hat{r} v_r) + \hat{r} R_4 \frac{\partial}{\partial \hat{z}} (\rho v_z) = 0 \tag{22}$$

$$\left(\frac{\rho}{\varepsilon}\right)\left[v_r\frac{\partial v_r}{\partial \hat{r}} + v_z\frac{R_4}{H}\frac{\partial v_r}{\partial z}\right] + \frac{\partial P}{\partial \hat{r}} - \mu\left[\frac{1}{R_4}\frac{\partial}{\partial \hat{r}}\left(\frac{1}{\hat{r}}\frac{\partial(\hat{r}v_r)}{\partial \hat{r}}\right) + \frac{R_4}{H^2}\frac{\partial^2 v_r}{\partial \hat{z}^2}\right] + \mu F R_4 v_r = 0 \tag{23}$$

and

$$\left(\frac{\rho}{\varepsilon}\right)\left[v_r\frac{H}{R_4}\frac{\partial v_z}{\partial \hat{r}} + v_z\frac{\partial v_z}{\partial z}\right] + \frac{\partial P}{\partial \hat{z}} - \mu\left[\frac{H}{R_4^2}\frac{1}{\hat{r}}\frac{\partial}{\partial \hat{r}}\hat{r}\left(\frac{\partial v_z}{\partial \hat{r}}\right) + \frac{1}{H}\frac{\partial^2 v_z}{\partial \hat{z}^2}\right] + \mu F H v_z = 0 \tag{24}$$

where the dimensionless variables are defined as

$$\hat{r} = \frac{r}{R_4};\ \hat{z} = \frac{z}{H} \tag{25}$$

In addition to the momentum conservation equations, an equation for pressure was required. Backstrom (9) derived this relationship for the case of fluid flow in an unfilled tube

$$\frac{1}{r}\frac{\partial}{\partial r}\left(r\frac{\partial P}{\partial r}\right) + \frac{\partial^2 P}{\partial r^2} + 2\rho\frac{v_r^2}{r^2} + w\left(\frac{v_r}{r} + \frac{\partial v_r}{\partial r} + \frac{\partial v_z}{\partial z}\right) = 0 \tag{26}$$

where w is an arbitrary constant used to enforce continuity.

The boundary conditions for the problem at hand along the $\hat{z} = 0$ and $\hat{z} = 1$ boundaries are

$$v_r = 0;\quad v_z = 0;\quad \frac{\partial P}{\partial z} = \frac{1}{r}\frac{\partial}{\partial r}\left(r\frac{\partial v_z}{\partial r}\right) + \frac{\partial^2 v_z}{\partial r^2} \tag{27}$$

Along the $\hat{r} = R_1/R_4$ boundary they are

$$\frac{\partial v_r}{\partial \hat{r}} = 0;\quad \frac{\partial v_z}{\partial \hat{r}} = 0;\quad P = P_{out} \tag{28}$$

and along the $\hat{r} = 1$ boundary they are:

$$\frac{\partial v_r}{\partial \hat{r}} = 0;\quad \frac{\partial v_z}{\partial \hat{r}} = 0;\quad P = P_{in} \tag{29}$$

where P_{in} and P_{out} are the inlet and outlet pressures (i.e., at $r = R_4$ and $r = R_1$), respectively.

EXPERIMENTAL APPARATUS AND PROCEDURE

A Superflo® 1500 radial-flow ion exchanger was purchased along with a support stand from Sepragen Corp. The solution (which was deionized water

initially) was withdrawn from a holding tank and pumped through the column using a Manostat Varistaltic® pump. Solution exiting from the column was returned to the holding tank. All plumbing was done with ¼-inch PVC plastic tubing. Dial pressure gauges, 0–30 psig, were mounted just before the inlet to the column and just after the discharge port. The inside and outside radii of the inner support tubes were 0.57 and 1.01 cm, respectively. The inside and outside radii of the outer support tubes were 4.29 and 4.60 cm, respectively. The height of the ion-exchange resin bed was 28.45 cm.

Fluid is introduced into the column through a very simple scheme. It is fed into a port in the center of the top support plate and then distributed to the gap between the outer support tube and the external structural support (in this case a clear plastic pipe) through 6 radial slots, each approximately ⅛-inch (3.2-mm) diameter. The effluent is collected from the interior of the inner support tube through a port centered in the bottom support plate.

To determine the relationship between pressure drop and flow rate, the desired flow rate was set on the pump and the pressure at both the inlet and discharge ports read from the pressure gauges after steady state had been reached, approximately 2 minutes. The actual flow rate was determined by collecting the discharged solution in a tared container for a measured time (typically 30 seconds). The mass of the solution was measured using an electronic balance and converted into a volumetric flow rate using published densities for water (10) at the measured solution temperature.

RESULTS AND DISCUSSION

To estimate the permeability and porosity of the support tubes, volumetric flow rate for several different pressure drops was collected without any ion-exchange resin in the column. This corresponds to the condition $\varepsilon_{ix} = 1$ and $F_{ix} = 0$. Shown in Fig. 2 are both the experimental results and a nonlinear least-squares fit of the data using the approximation of an infinitely long column, i.e., Eqs. (17)–(21). The results of the nonlinear least-squares analysis gave the "best fit" with $\varepsilon_s = 0.0023$ and $F = 8.48 \times 10^4$ cm^{-2}.

To test the accuracy of the finite-element analysis (FEA), two test cases were evaluated. The first corresponded to radial flow in an infinitely long tube without any packing or supports. The operating conditions for this case were a pressure drop of 200 dynes/cm^2 (this value was selected so the velocities were approximately equal to those determined for the data shown in Fig. 3), a fluid viscosity of 0.01 poise, and a fluid density of 1.0 gm/cm^3. In terms of the discussion above, this is equivalent to the case of $\varepsilon_s = \varepsilon_{ix} = 1$ and $F_s = F_{ix} = 0$ and using symmetry boundary conditions at $\hat{z} = 0$ and $\hat{z} = 1$. The analytical solution for this problem is given by Bird et al. (7).

The second test of the FEA simulation was the infinitely long, layered column whose solution is given above for a pressure drop of 10^5 dyne/cm^2 and

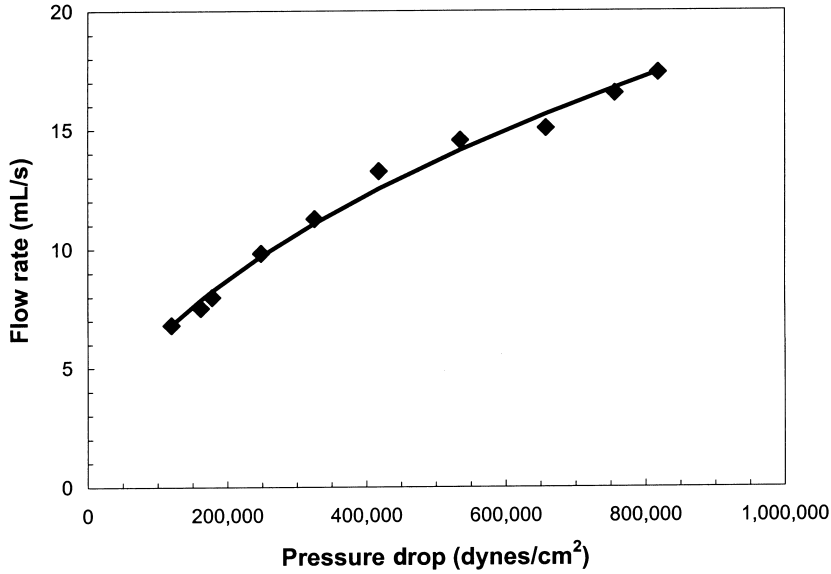

FIG. 2 Comparison of experimental (symbols) and calculated (solid curve) volumetric flow rates for the layered-cylinder model.

the same fluid properties as above. For this case, the porosity of the support tubes and the ion-exchange resin were selected to be

$$\varepsilon_s = 0.0023;\ \varepsilon_{ix} = 0.20 \tag{30}$$

while their permeabilities were chosen as

$$k_s = k_{ix} = 10^{-5}\ \text{cm}^2 \tag{31}$$

These values were selected to ensure the stability of the FEA simulation.

The agreement between the FEA model and the analytical solutions (Fig. 3) was satisfactory. In fact, the root mean square of the difference between the analytical solution and the FEA calculations for the radial velocity and pressure profiles for the second simulation were 8.4×10^{-5} and 2.9×10^{-6}, respectively.

Two simulations were conducted on finite-length columns. The first corresponded to a completely filled column, i.e., one in which the ion-exchange resin extended to the top of the column, and the second to one in which the ion-exchange resin only filled 98% of the available space. This corresponds to an empty headspace of 0.56 cm in the actual column. For both studies, the values for the porosities and the permeabilities of the support columns and the resin given above were used. For the second case, in the unfilled region the

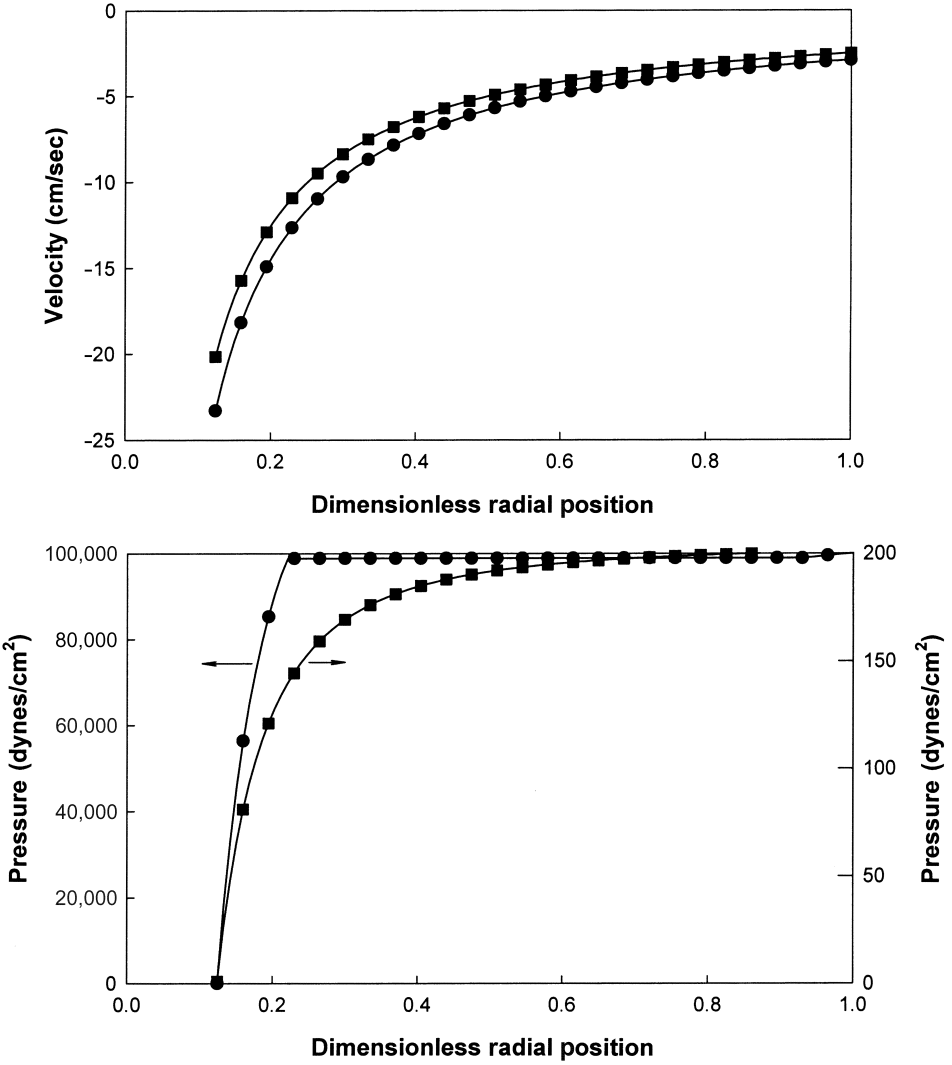

FIG. 3 Comparison of FEA results (symbols) and analytical models (solid curves) for an infinitely long column. The squares are results for an isotropic cylinder ($\varepsilon_s = \varepsilon_{ix} = 1.0$, $F_s = F_{ix} = 0.00\ \text{cm}^{-2}$); the circles are results for the layered-cylinder model ($\varepsilon_s = 0.0023$, $F_s = 0.0\ \text{cm}^{-2}$, $\varepsilon_{ix} = 0.2$, $F_{ix} = 10^5\ \text{cm}^{-2}$).

values of $\varepsilon_u = 1.0$ and $F_u = 0.0$ were used. For both cases, an applied pressure across the column of 1×10^5 dynes/cm^2 was used. This resulted in radial velocities at the inner and outer radii of the column of -21 cm/sec and -2.6 cm/sec, respectively. The same permeabilities and porosities used above were used in these simulations.

For the completely filled column (Fig. 4), the expected behavior was observed. Adjacent to the top and bottom walls (only the top 10% of the column is shown in Fig. 4 for clarity) symmetric boundary layers were observed. These boundary layers occupied approximately 1% of the top and bottom of the column with a distinct demarcation between the boundary layer and the bulk flow region at a constant distance from the solid wall. Based on these results, the flow rate through the column could easily be approximated by the layered cylinder model. Furthermore, since the velocities in boundary layer are less than in the bulk, the presence of this boundary layer would make predictions of contaminant breakthrough based on the layered-cylinder model conservative estimates.

Through the bulk of the column the flow is laminar (Fig. 5) with the modified Reynolds number (see Eq. 5) ranging between 360 and 1500. However, in the support columns, the modified Reynolds number is much larger, rang-

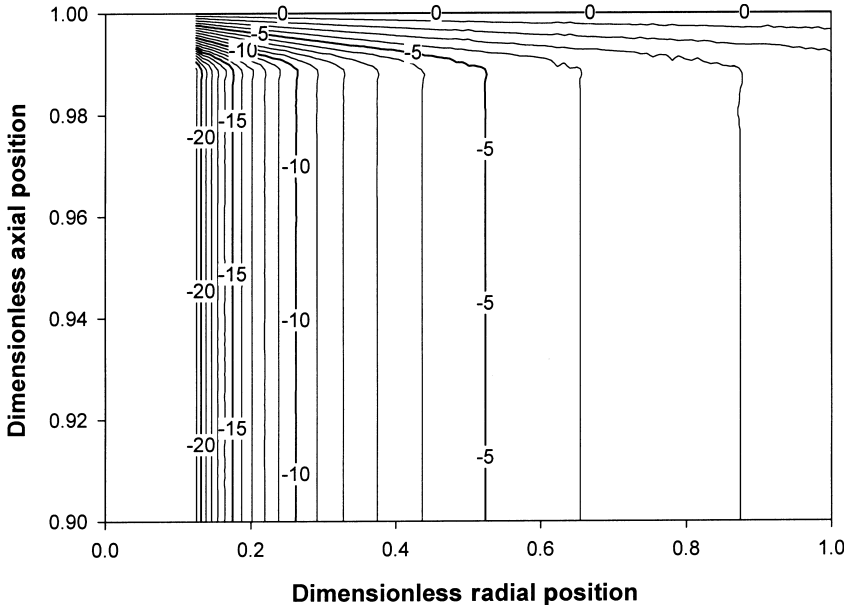

FIG. 4 Radial velocity profiles for the top 10% of a finite height column that is completely filled with resin.

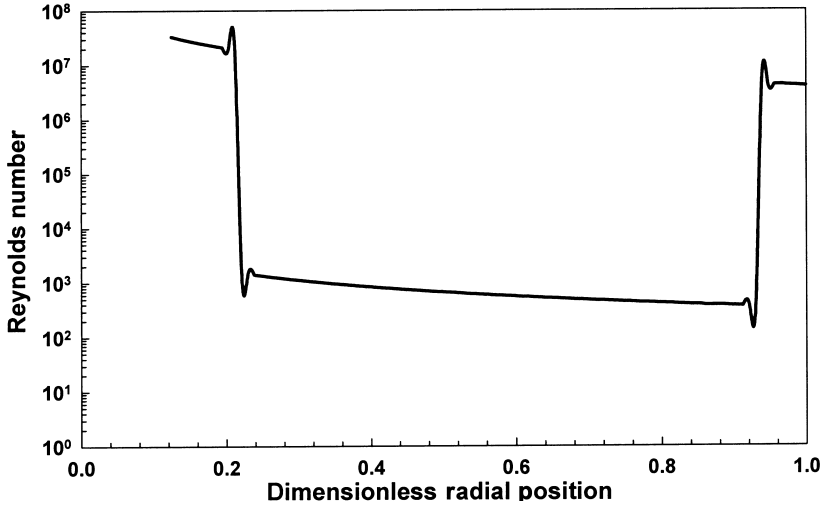

FIG. 5 Reynolds number for the flow conditions in Fig. 4.

ing between 4×10^6 and 3×10^7. This is due to the much lower assumed porosity in the support structures and causes the value of the shear factor to be underestimated. Since interest was in the flow in the column, this is not a serious problem.

The case of the partially filled column (Fig. 6, where again only the top 10% of the column is shown) is much more interesting. At a constant radial position, the velocity in the boundary layer, instead of monotonically increasing from the imposed zero velocity at the wall to the bulk flow velocities, goes through a maximum before returning to the bulk flow velocity near the top of the packing. This behavior is observed in the support columns as well.

The velocities in the empty headspace are not as high as would be predicted by the layered-cylinder model for an infinitely long, empty column, reflecting the effects of both the solid wall and the constrained velocity in the ion-exchange resin. In terms of estimating the efficiency of this column, however, it must be remembered that the volumetric flow through the headspace per unit height will be greater than that through the ion-exchange resin because of the higher velocities as well as the differences in porosity. The ion-exchange resin porosity being only 0.20 compared to 1.0 in the headspace, means that even at the same velocities, five times more fluid will flow through the headspace as through an equivalent height of ion-exchange resin. This means that in the current column, with only a 0.56 cm unfilled headspace, approximately 9% of the

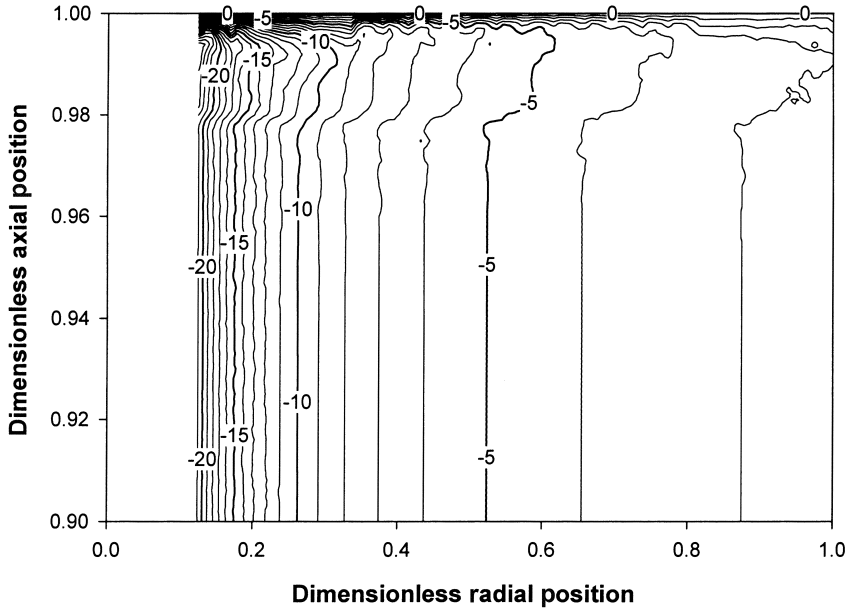

FIG. 6 Radial velocity profiles for the top 10% of a finite column of which only 98% is filled with resin.

feed solution would not pass through the resin bed at all and would be untreated.

Yoo and Dixon (11) and Zardi and Bonvin (12) describe a method to prevent unreacted feed gases from exiting from the top of a combined axial- and radial-flow catalytic bed. They used a nonporous containing-wall section at the top of the catalyst bed to ensure that all the reactants passed through the bed before exiting from the reactor. To determine if the same approach would be effective in the current situation, a simulation was conducted in which the top 10% of the inner and outer support columns were nonporous, and the top 2% of the resin bed was unfilled. The other flow conditions were the same as the prior simulations when there was an empty headspace above the bed. The results (Fig. 7) indicate that the use of the nonporous wall sections causes a stagnant pool of liquid to saturate the top portion of the bed. In this stagnant region there is essentially no flow through the portion of the bed between the nonporous portion of the supports and no radial flow at all through the empty headspace. Although adding the nonporous section decreases the effective height of the ion-exchange column, the improvement in the efficiency of contaminant removal would more than offset this problem.

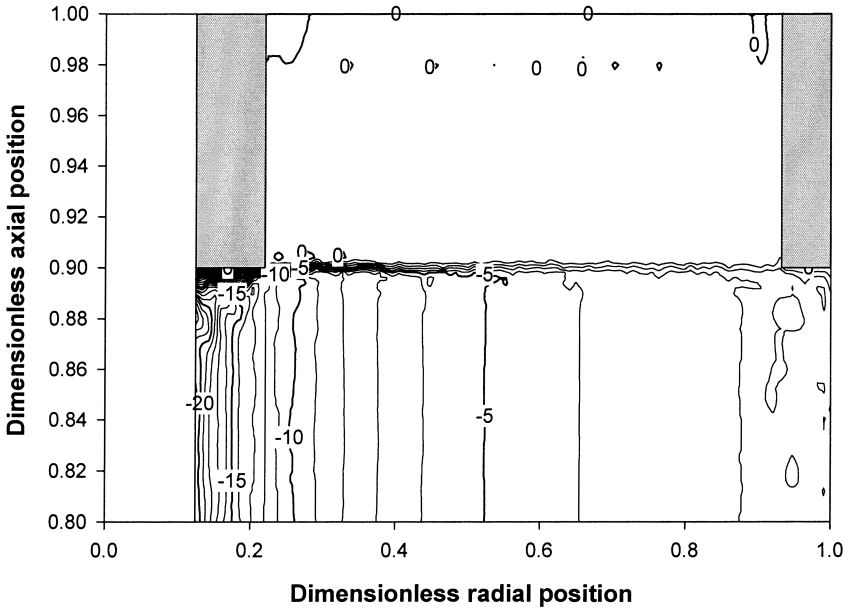

FIG. 7 Radial velocity profile for the top 20% of a finite column of which only 98% is filled with resin, and the top 10% of the supports are impermeable (indicated by the gray shaded area). Flow conditions are described in the text.

Conclusions and Recommendations

Because of the high possibility of not completely filling the column with ion-exchange resin and the resulting bypass of the resin bed by the contaminated fluid, this geometry does not seem suitable for applications in which removal of the contaminant is absolutely necessary, such as with removal of radioactive contaminants. Based on the results presented in this report, the following conclusions and recommendations are made:

- The fluid dynamics of an infinitely tall, radial-flow ion-exchange column can be adequately modeled using the layered-cylinder model.
- Finite-element analysis can be used to determine the flow patterns in finite-height columns, completely filled as well as partially filled ones.
- Analysis of partially filled columns demonstrates that even if only a small percentage of the column is unfilled, unacceptable amounts of the contaminated fluid will bypass the resin and be discharged from the unit untreated—an exaggeration of channeling along the walls in an axial-flow column.
- Making the top 10% of the support membranes impermeable will eliminate the problem of overflow in an unfilled column.

ACKNOWLEDGMENTS

The author is grateful to Dr. Keith Fife, Nuclear Materials Technology Division, Los Alamos National Laboratory, Los Alamos, NM, for encouragement and financial support during the completion of this project. In addition, several undergraduate students assisted in the assembly of the laboratory apparatus and data acquisition, including Johnny Flores, Kimber Rawdon, Wendal Salas, and April Smith.

REFERENCES

1. L. Lapidus and N. R. Amundson, "Mathematics of adsorption in beds. III. Radial flow," *J. Physical Chem., 54,* 821–829 (1950).
2. L. Lapidus and N. R. Amundson, "The rate-determining steps in radial adsorption analysis," *Ibid., 56,* 373–383 (1952).
3. Y. Tsaur and D. C. Shallcross, "Modeling of ion exchange performance in a fixed radial flow annular bed," *Ind. Eng. Chem. Res., 36,* 2359–2367 (1997).
4. Y. Tsaur and D. C. Shallcross, "Comparison of simulated performance of fixed ion exchange beds in linear and radial flow," *Solvent Extr. Ion Exch., 15*(4), 689–708 (1997).
5. J. P. Tharakan and M. Belizaire, "Protein band dispersion in axial and radial flow chromatography," *J. Liq. Chromatogr., 18*(1), 39–49 (1995).
6. S. Liu and J. H. Masliyah, "Principles of single-phase flow through porous media," in *Suspensions: Fundamentals and Applications in the Petroleum Industry* (L. L. Schramm, Ed.), *Advances in Chemistry Series 251,* American Chemical Society, Washington, DC, 1996.
7. R. B. Bird, W. E. Stewart and E. N. Lightfoot, *Transport Phenomena,* Wiley and Sons, New York, 1960.
8. *PDEase2,* Macsyma, Inc., Arlington, MA, 1998.
9. G. Backstrom, *Fields of Physics on the PC by Finite Element Analysis,* 2nd ed., Studentlitteratur, Lund, Sweden, 1996.
10. R. Perry, *Perry's Chemical Engineering Handbook,* 6th ed., McGraw-Hill, New York, 1984.
11. C.-S. Yoo and A. G. Dixon, "Modeling and simulation of a mixed-flow reactor for ammonia and methanol synthesis," *Chem. Eng. Sci., 43,* 2859–2865 (1988).
12. F. Zardi and D. Bonvin, "Modeling, simulation and model validation for an axial-radial ammonia synthesis reactor," *Chem. Eng. Sci., 47,* 2523–2528 (1992).

Received by editor March 23, 1999
Revision received March 2000